

# Development of Tensile Hoop Stress during Horizontal Directional Drilling through Sand

Matthew J. Kennedy<sup>1</sup>; Ian D. Moore, M.ASCE<sup>2</sup>; and Graeme D. Skinner<sup>3</sup>

**Abstract:** Although horizontal directional drilling has become commonplace, there are problems associated with high drilling mud pressures causing hydraulic fracture leakage of mud out into the environment. Initiation of tensile fracture is examined here, using finite-element analysis to represent the sand material and the annulus of filtercake that forms around the borehole. The analyses examine the soil response as mud pressures are increased, including shear failure in the sand material and the cohesive filtercake layer. The study identifies the initial geostatic stress conditions and the drilling fluid pressures that initiate tensile stresses in the filtercake. The effects of filtercake thickness, borehole depth, and the location of the maximum tensile stresses are studied. Significant discrepancies are found relative to limits currently used in the industry. Tensile fracture may be responsible for some mud loss, but simple use of drilling mud pressures that prevent tensile circumferential stress may be overly conservative.

**DOI:** 10.1061/(ASCE)1532-3641(2006)6:5(367)

**CE Database subject headings:** Trenchless technology; Drilling; Finite element method; Sand; Tensile stress.

## Introduction

Horizontal directional drilling (HDD) has been used in practice since the late 1970s. First employed in the oil and gas industries, HDD was only adapted for use in smaller municipal applications in the mid 1980s (Arairatnam et al. 1999). The underground conduit installation technique belongs to a family of construction practices known as “trenchless technologies.” The North American Society of Trenchless Technology defines these techniques as means for “utility line installation, replacement, rehabilitation, renovation, repair, inspection, location and leak detection, with minimum excavation from the ground surface” (NASTT 2001). By utilizing these techniques, installation and repair of buried sewer, water, and other utility conduits can be achieved at a far cheaper cost than with existing open-cut methods. Not only will the time and costs associated with planning and construction be reduced, the implementation of many of these techniques will go relatively unnoticed to the public or local business.

HDD employs drilling slurry during all stages of the construction process. This slurry aids in cooling of the cutting head, reduction of shear resistance along the borehole wall, transport of soil cuttings, as well as some additional borehole structural sup-

port. The magnitude of the drilling slurry pressure in the borehole affects a problem commonly encountered known as “frac-out” or “hydraulic fracture.”

Kennedy et al. (2004a) examined the response of cohesive soil during directional drilling under a range of different drilling slurry pressures. Assuming a tensile strength for clay of zero, they found that when soil response is elastic, the mud (drilling fluid) pressure  $P_{\max}$ , where compressive stresses decrease to zero at the crown of the borehole and tensile fractures, may initiate is given by

$$P_{\max} = \sigma_0(3K_0 - 1) \quad (\text{for } K_0 < 1) \quad (1)$$

where  $\sigma_0$ =overburden pressure at the level of the crown prior to drilling and  $K_0$ =coefficient of lateral earth pressure at rest. Kennedy et al. (2004b) examined the nonlinear response of purely cohesive soils, and demonstrated that for very low mud pressures, shear failure develops in the soil at the crown of the cavity as the cavity collapses inward, with circumferential stress  $\sigma_\theta$  given by radial mud pressure  $\sigma_r$  and undrained cohesion of the clay  $c_u$

$$\sigma_\theta = \sigma_r + 2c_u \quad (\text{for } \sigma_r < \sigma_\theta) \quad (2)$$

For high mud pressures, the cavity expands outwards, at which point

$$\sigma_\theta = \sigma_r - 2c_u \quad (\text{for } \sigma_r > \sigma_\theta) \quad (3)$$

Naturally, the soil response when drilling through sand will be very different. Because sand is a porous material, it allows the drilling slurry to infiltrate a thin annular layer around the borehole creating a composite layer of sand and drilling slurry known as the “filtercake.” This layer helps to reduce seepage loss of drilling slurry and aids in the support of the borehole. It greatly affects the behavior of the sand system during the HDD process. An understanding of the sand-filtercake system response to the HDD process is needed to establish how drilling slurry pressures initiate hydraulic fracture.

<sup>1</sup>Geotechnical Engineer in Training, Golder Associates, 500-4260 Still Creek Dr., Burnaby BC, Canada V5C6C6. E-mail: mkennedy@golder.com

<sup>2</sup>Professor and Canada Research Chair in Infrastructure Engineering, GeoEngineering Centre at Queen's-RMC, Queen's Univ., Kingston ON, Canada K7L 3N6 (corresponding author). E-mail: moore@civil.queensu.ca.

<sup>3</sup>Geotechnical Engineer, Golder Associates, 10th Floor, 940 6th Ave. S.W., Calgary AB, Canada T2P 3T1. E-mail: gskinner@golder.com

Note. Discussion open until March 1, 2007. Separate discussions must be submitted for individual papers. To extend the closing date by one month, a written request must be filed with the ASCE Managing Editor. The manuscript for this paper was submitted for review and possible publication on September 24, 2004; approved on March 18, 2005. This paper is part of the *International Journal of Geomechanics*, Vol. 6, No. 5, October 1, 2006. ©ASCE, ISSN 1532-3641/2006/5-367-373/\$25.00.

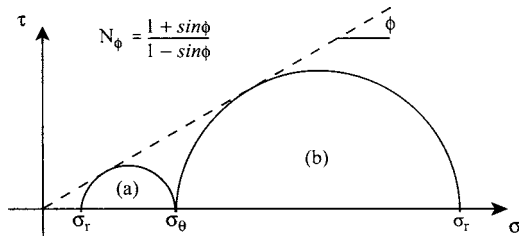


**Fig. 1.** Mohr-Coulomb failure plot for soil with cohesion equal to zero

The equation currently available to designers to predict the maximum allowable drilling slurry pressure ( $P_{\max}$ ) to avoid mud loss in both sand and clay was developed at the Delft University of Technology and is (Arends 2003)

$$P_{\max} = (p'_f + c \cot \phi) \left\{ \left( \frac{R_0}{R_{p,\max}} \right)^2 + Q \right\}^{-\sin \phi / (1 + \sin \phi)} - c \cot \phi \quad (4)$$

where  $p'_f = \sigma'_0(1 + \sin \phi) + c \cos \phi$ ;  $c$ =cohesion;  $\phi$ =internal friction angle;  $\sigma'_0$ =initial effective stress;  $R_0$ =initial radius of the borehole;  $R_{p,\max}$ =maximum allowable radius of the plastic zone;  $Q = (\sigma'_0 \sin \phi + c \cos \phi) / G$ ; and  $G$ =shear modulus. This equation was developed for isotropic soils, assumes the lateral earth pressure coefficient at rest ( $K_0$ ) is unity, and neglects geostatic stress distributions in the vicinity of the borehole. It examines the ring of soil around the borehole undergoing shear failure at high values of mud pressure, and keeps the radius of that zone of elastoplastic soil below the ground surface. It also does not consider the failure mechanism examined by Kennedy et al. (2004a,b), namely, tensile fracture of the soil.

Wang and Sterling (2004) also studied shear failure around the borehole during directional drilling, using numerical analyses to quantify plastic yielding of the sand. They concluded that this type of shear failure generally precedes initiation of slurry loss, and that a suitable drilling fluid pressure would be equal to the maximum earth pressure.

The purpose of the present study is to examine the effect of mud pressures on circumferential stresses adjacent to the borehole when horizontal directionally drilling through a sand-filtercake system. Finite element analysis is used, extending the procedures developed by Kennedy et al. (2004a,b). The study establishes a typical set of soil parameters for sand and filtercake, then examines how mud pressures, filtercake thickness and other factors influence the potential initiation of tensile fracture in the soil. The work concludes with a discussion of the finite element results in the context of the existing literature.

## Plasticity Theory Review

When yielding occurs in the host soil adjacent to the borehole, the stresses are compared with those specified by a Mohr-Coulomb failure criterion. For a purely frictional material, there is no cohesion and the shear strength is governed by the principal stresses at the point of failure (Fig. 1).

The radial stress ( $\sigma_r$ ) at the borehole periphery is equal to the pressure applied by the drilling slurry inside the borehole ( $P_f$ ). The major and minor principal stresses will be equal to the tangential or radial stresses at this boundary depending on the situation. When the drilling slurry pressure is low, the radial

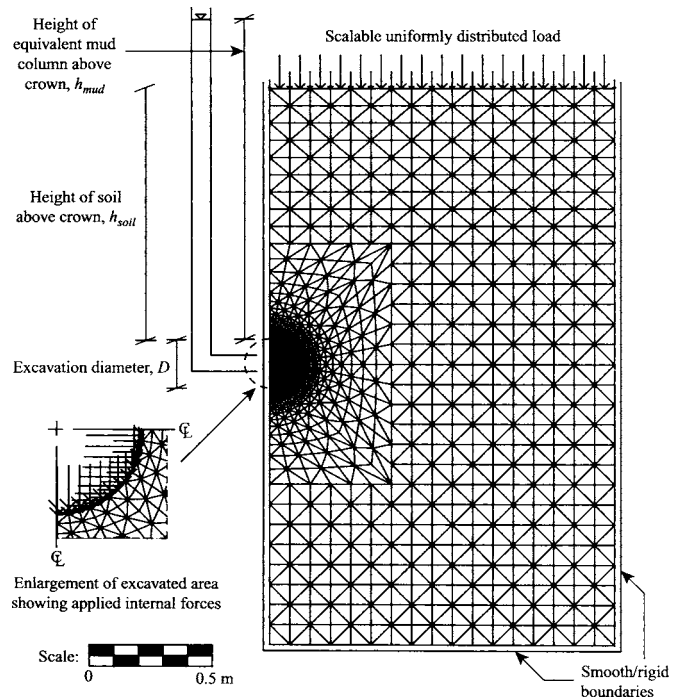


**Fig. 2.** Example mesh and parameter definition

stress is the minor principal as it is less than the tangential stress [Fig. 1(a)]. When the drilling slurry pressure is high, the radial stress is the major principal since it is greater than the tangential stress [Fig. 1(b)]. From the geometry of the Mohr-Coulomb plot in Fig. 1 the quotient of the major and minor principal stresses ( $N_\phi$ ) can be described in terms of the friction angle. Therefore the Mohr-Coulomb failure of a purely frictional material can be written as

$$\sigma_\theta = \sigma_r N_\phi \quad (\text{for } \sigma_r < \sigma_\theta) \quad (5)$$

$$\sigma_\theta = \frac{\sigma_r}{N_\phi} \quad (\text{for } \sigma_r > \sigma_\theta) \quad (6)$$

## Preliminary Discussion of Numerical Modeling

Because the current state-of-the-art design equation [Eq. (4)] was developed for isotropic initial stress conditions, it considers a  $K_0$  of unity. This is a significant approximation as normally consolidated sands generally exhibit  $K_0$  values between 0.35 and 0.5 (Holtz and Kovacs 1981). Eq. (4) also neglects gravity effects (i.e., gradients of stress with depth). Finite element analysis is able to consider a general value of  $K_0$  as well as gradients of earth pressure and drilling slurry pressure due to gravity. The finite element mesh employed for this research also attempts to minimize the effects of model boundaries on the analysis results that may have occurred in previous finite element modeling of the problem where the zone of shear failure reached the mesh boundaries (Wang and Sterling 2004).

The finite element analysis employed here is based on the approach used earlier by Kennedy et al. (2004a,b) to investigate directional drilling through clay soil. To model a cross section during the construction process, it is examined under two-dimensional, plane-strain conditions. As shown in Fig. 2, the mesh becomes finer near the area that becomes the borehole

around which the critical stresses develop. Smooth, rigid boundaries were placed along the bottom and sides of the mesh and along the vertical borehole axis (a line of symmetry). The bottom and remote side boundary were placed a sufficient distance from the borehole to ensure that stresses along these boundaries remain close to geostatic stress conditions. Kennedy et al. (2004a) established that this finite element mesh containing 1,804 six-noded triangular elements gives stress values in the vicinity of the borehole that are within 1% of those from the elastic plate theory of Obert and Duval (1967). In addition to a convergence check undertaken to confirm that the level of mesh refinement is adequate for inelastic analysis (results not presented here), subsequent discussion demonstrates that the results match closed form results for the case of the “sand alone” condition.

The analysis models elastoplastic constitutive behavior based on the Mohr-Coulomb failure criterion. Although the use of a dilation angle equal to the angle of friction will overestimate dilation in sands subjected to significant levels of shear strain, an associated flow rule was employed, given the benefits to numerical stability and the limited zone of shear failure that develops adjacent to the borehole. Previous experience with tunneling and buried pipe analyses featuring static (not kinematic) boundary conditions demonstrates that the stress state in the vicinity of the borehole is essentially unaffected by the dilation angle, Moore and Booker (1987).

A uniformly distributed load is placed along the top surface to represent the overlying soil when the construction is to take place at a depth larger than the height of elements above the crown of the borehole. This overburden pressure is scaled to represent various depths of construction and is placed a sufficient distance away to ensure that the stiffness of the soil above the top of the mesh can be neglected without affecting the soil stresses around the borehole. The initial geostatic pressures in the soil are defined using the unit weight of the sand ( $\gamma_{\text{soil}}$ ) and  $K_0$ .

As it is not feasible to model every aspect of the drilling process, a simplified two-dimensional representation is used. The equivalent nodal forces along the inside of the borehole annulus that represent the reactions due to the soil under initial geostatic conditions are calculated using a separate finite element analysis. A similar set of equivalent nodal forces is calculated for each value of final drilling slurry pressure (at the end of borehole construction) considered in the parametric study. A multistep, linear interpolation from the initial force set to the final is then used to model the stress path beginning with initial geostatic soil stresses and ending with the drilling slurry pressure. The number of load steps used to undertake this progressive change in nodal forces was increased until the final stress state converged to a consistent result. This simple stress path considers the simultaneous, combined removal of the host soil and application of slurry pressures in the borehole. Clearly it is a “first approximation” representation of the drilling process that avoids consideration of the complexities of the cutting process, and the three-dimensional advance of drilling string.

The analysis does not consider temperature, chemical, seepage, or other time-dependent effects of the sand-slurry interaction to create the filtercake. At the beginning of the modeled drilling process, the material properties of a ring of model elements around the borehole were changed to those of the filtercake. These material properties do not subsequently change; therefore, the filtercake is modeled as present throughout the construction process.

Filtercake thickness can be influenced by the composition of the drilling slurry (Edil and Muhanna 1992). However in

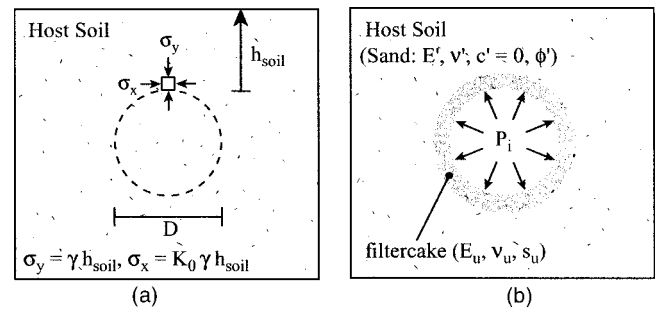


Fig. 3. Soil conditions (a) before; (b) after HDD through sand

most publications the filtercake is generally taken to be between 1 and 3 cm thick (Arends 2003; Edil and Muhanna 1992; Wang and Sterling 2004). The sensitivity of the results to filtercake thickness was studied using analyses with filtercake thicknesses of 0.93, 2, 7, and 15 cm.

## Material Modeling

### Sand

Medium sand was chosen as the host soil, having a unit weight of  $20 \text{ kN/m}^3$ , friction angle of  $35^\circ$ , and a  $K_0$  of 0.4 [using Jaky's equation (Holtz and Kovacs 1981)]. These parameters control both the initial geostatic stresses in the soil, as well as the drained response of the sand in the sand-filtercake system. The drained elastic modulus of the sand ( $E'$ ) and Poisson's ratio were taken as 18 MPa and 0.3, respectively.

The sand is analyzed using effective stress analysis with pore pressures set to zero. This effectively represents borehole construction above the water table. For sites with a high water table, the effective stresses being considered here would correspond to deeper construction, neglecting the small effects of earth pressure gradients across the borehole (double the depth if groundwater level is at the ground surface).

### Filtercake Parameters

Because the filtercake would be composed of drilling slurry that had infiltrated the sand material, its unit weight was assumed equal to that of the host sand— $20 \text{ kN/m}^3$ . Any increase in unit weight in this thin zone of material can be expected to have a negligible impact on the behavior.

The bentonite drilling slurry filling the sand pores within the filtercake substantially lowers the permeability. In contrast to the purely frictional “host” sand, the filtercake is modeled as exhibiting undrained behavior. The selection of undrained strength and deformation parameters is made considering the relationship between this “new” slurry-sand composite, and the original sand. Fig. 3(a) shows the initial conditions in the sand in the vicinity of the borehole. Fig. 3(b) shows the drilled cavity and the undrained filtercake material layer between the borehole and the drained, frictional sand.

Though it exhibits undrained responses, the filtercake strength parameters are still largely based on the frictional strength of its sand component. Consideration of the changes in mean stress can indicate the development of excess pore pressures. For elastic soil response, the increase in borehole pressure (radial stress applied by the mud at the outer boundary of the borehole) results in an

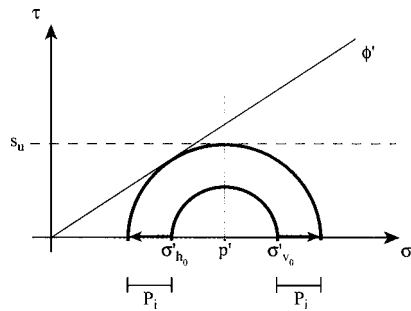


Fig. 4. Mohr-Coulomb failure plot of filtercake material

equal and opposite reduction of the tangential stress around the borehole (e.g., Hefhy and Lo 1992). The change in mean total stress if filtercake response is elastic is therefore zero,  $\Delta p=0$ .

Because the filtercake exhibits undrained response with no volume change, the mean effective stress in the filtercake at the crown of the borehole also remains constant (Fig. 4,  $\Delta p'=0$ ). Excess pore pressures are therefore zero, and the undrained shear strength of the filtercake will be half the principal stress difference at the point of first yield of the sand constituent. The filtercake (FC) therefore has undrained shear strength based on the initial frictional strength of the sand particles. From Fig. 4, the undrained shear strength ( $s_u$ ) is calculated as

$$(S_u)_{FC} = \frac{1}{2} \sigma'_{v0} (1 + K_0) \sin \phi' \quad (7)$$

The filtercake is therefore modeled as a purely cohesive material. Given the small change in initial effective stress from the crown to the invert of the borehole, a single value of undrained cohesion obtained using Eq. (7) and  $\sigma'_{v0}$  evaluated at the crown is employed.

Eq. (7) provides values of filtercake shear strength very similar to those in the literature. The filtercake shear strength chosen by Wang and Sterling (2004) for their finite element analyses of a sand-filtercake system and that calculated for the same system by Eq. (7) differ by less than 2%.

An approximate value of the drained elastic modulus of the sand is chosen considering the soil as a well graded sand (SW according to the Unified Classification System) at density of 80% of the maximum density achieved in a standard Proctor test (this is consistent with the friction angle of  $35^\circ$  and the unit weight of  $20 \text{ kN/m}^2$ ). Based on the database of Selig (1988), the drained modulus at the shallowest and deepest configurations being examined would only vary by about 20%. Therefore, because local stress and strength is the focus of this study, the drained modulus was modeled as constant for all depths examined, avoiding unnecessary complication. The elastic parameters of the filtercake were estimated by assuming its undrained shear modulus is equal to the drained shear modulus of the sand. All the material properties used for the modeling of the HDD process in medium sand are listed in Table 1.

Table 1. Material Parameters for Sand-Filtercake Soil-System Model

Sand		Filtercake	
Drained elastic modulus, $E'$	18 MPa	Undrained elastic modulus, $E_u$	21 MPa
Poisson's ratio, $\nu'$	0.3	Poisson's ratio, $\nu_u$	0.4999
Cohesive strength, $c'$	0	Shear strength, $s_u$	[Eq. (7)]
Friction angle, $\phi'$	$35^\circ$	Friction angle, $\phi$	0

## Drilling Mud

The only parameter considered for the drilling mud is the unit weight, a value assumed throughout as  $13 \text{ kN/m}^3$ . All calculations are presented in terms of the mud pressure at the crown, springline or invert, so results are expected to be very close to those for mud with other values of unit weight. The changes associated with higher or lower gradients across the borehole are expected to be negligible.

## Finite-Element Analysis Results

### Model Evaluation and Boundary Effects

The mesh used here was adapted from that used by Kennedy et al. (2004a,b) in their earlier studies of drilling through cohesive soils. The proximity of the mesh boundaries was examined. These boundaries should be a sufficient distance from the borehole to maintain stress profiles at those boundaries at the end of construction that are similar to geostatic (preconstruction) stresses. They also need to be remote from zones exhibiting nonlinear soil response (the regions of shear failure). Differences in stresses along the remote side boundary and the bottom boundary before and after borehole excavation were less than 5 and 2%, respectively—both considered to be acceptable given the negligible effect on stresses at the borehole expected as a result of these small discrepancies at those boundaries.

### Sand Analysis

To gain a better understanding of the response of the soil-filtercake system to the horizontal drilling process, finite element analyses were performed to examine a soil system composed of sand only. An evaluation of the annular tangential stresses around the borehole revealed that the minimum (least compressive) tangential value could occur at either the crown or the invert. Fig. 5 compares the tangential stress at the borehole crown calculated using elastic theory [Eq. (1)], plasticity theory for a purely frictional material [Eqs. (5) and (6)], and that at the crown and invert calculated using finite element analysis for construction at a depth of 5 m. Results are presented for a range of final drilling slurry pressures.

At lower slurry pressures (Fig. 5,  $P_i < 10 \text{ kPa}$ ), the plasticity solution in Eq. (5) predicts the tangential crown stress from the finite element analyses well. Similarly, at higher slurry pressures (Fig. 5,  $P_i > 32 \text{ kPa}$ ), the plasticity solution in Eq. (6) matches the finite element results. As expected, the tangential stresses at the invert are slightly higher than those at the crown due to gradients with depth over the diameter of the borehole. However, unlike the fine-grained analyses reported by Kennedy et al. (2004b), the tangential crown stress at intermediate drilling slurry pressures (Fig. 5,  $10 \text{ kPa} < P_i < 32 \text{ kPa}$ ) is not well predicted by elastic

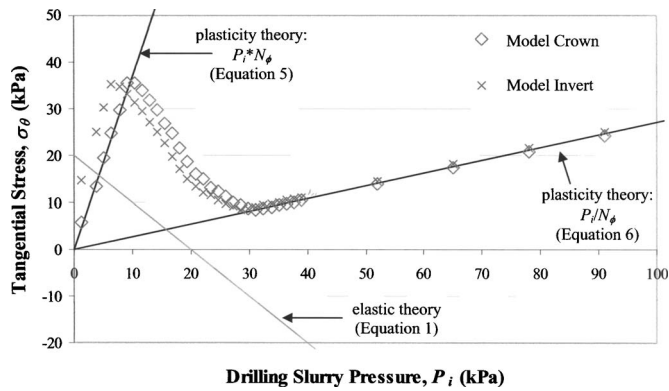


**Fig. 5.** Tangential stress at crown from elastic theory, plasticity theory, and at crown and invert from finite element analyses [ $h_{\text{soil}}=5$  m,  $\gamma_{\text{soil}}=20$  kN/m<sup>3</sup>,  $K_0=0.4$ ,  $\phi=35^\circ$ ,  $\gamma_{\text{mud}}=13$  kN/m<sup>3</sup>, and  $(s_u)_{\text{FC}}=40$  kPa]

theory. Even though there is an elastic response at the crown of the borehole when an intermediate drilling slurry pressure is employed, the complex plasticity distribution further away from the borehole where shear failure has already occurred influences the tangential crown stress, so it remains above the value predicted by elastic theory (Fig. 5). The analyses in Fig. 5 show that the critical (least compressive) annular tangential stress for the intermediate drilling slurry pressures occurs at the invert of the borehole, not at the crown.

Fig. 6(b) shows this plastic zone when a drilling slurry in this range is employed and the region of the material responding elastically near the crown. Fig. 6 also illustrates the location of plastic zones (regions of shear failure) around the borehole for low [Fig. 6(a)] and high [Fig. 6(c)] drilling slurry pressures.

### Sand-Filtercake System Analysis

In the analyses modeling the same range of drilling slurry pressures for a sand-filtercake system, the filtercake material around the borehole periphery controls the crown stress. Fig. 7 compares the tangential stress at the borehole crown calculated using elastic theory [Eq. (1)], purely cohesive plasticity theory [Eqs. (2) and

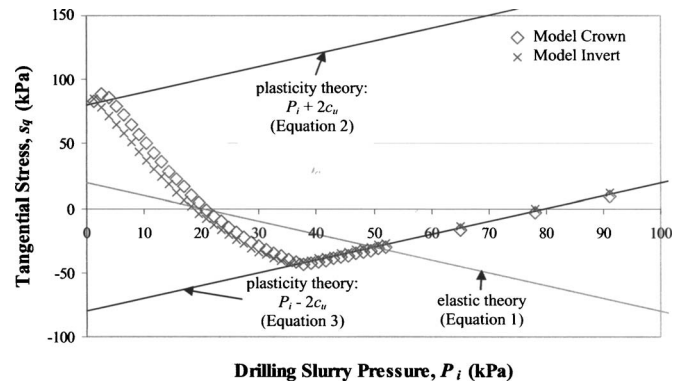


**Fig. 7.** Tangential stress at crown from elastic theory, plasticity theory, and at crown and invert from finite element analyses with a 2 cm thick filtercake layer [ $h_{\text{soil}}=5$  m,  $\gamma_{\text{soil}}=20$  kN/m<sup>3</sup>,  $K_0=0.4$ ,  $\phi=35^\circ$ ,  $\gamma_{\text{mud}}=13$  kN/m<sup>3</sup>, and  $(s_u)_{\text{FC}}=40$  kPa]

(3)] and those at the crown and invert calculated using finite element analysis for borehole construction at a depth of five metres featuring a 2 cm thick layer of filtercake.

For very small drilling slurry pressures (Fig. 7,  $P_i < 4$  kPa), the tangential stress at the crown of the borehole is approximately given by the plasticity theory for a purely cohesive material presented by Kennedy et al. (2004a), Eq. (2), based on the material properties of the filtercake. Similarly, for large drilling slurry pressures (Fig. 7,  $P_i > 38$  kPa), it is effectively calculated using plasticity theory for cohesive soil, Kennedy et al. (2004a), Eq. (3). As in the pure sand analysis where the soil response is predicted by plasticity theory, the tangential stresses at the invert are slightly higher than at the crown. Again, with intermediate drilling slurry pressures (Fig. 7,  $4$  kPa  $< P_i < 38$  kPa), the tangential stress at the crown is not reliably predicted by elastic theory [Eq. (1)] and critical stresses occur at the invert. This lack of agreement with elastic theory can be attributed to shear failure in the sand affecting the stresses near the crown of the borehole (Fig. 8).

Where Fig. 7 and some subsequent figures show tensile (negative) circumferential stresses, there is a possibility of tensile fracture. The approach taken in the earlier work (Kennedy et al. 2004b) has been to identify when fracture may occur, based on a

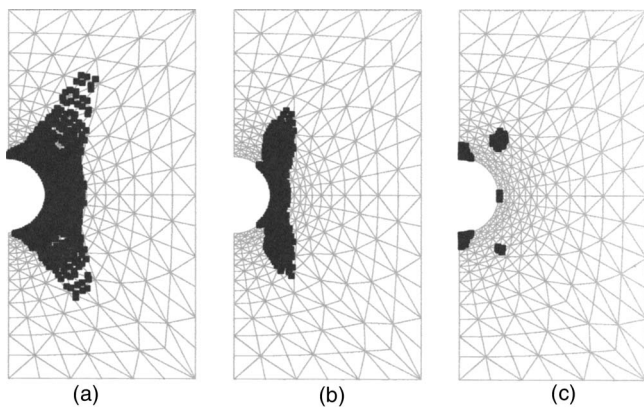


**Fig. 6.** Yielded plastic zones from finite analyses of pure sand system for drilling slurry pressure of (a) 7.8; (b) 19.5; and (c) 52 kPa [ $h_{\text{soil}}=5$  m,  $\gamma_{\text{soil}}=20$  kN/m<sup>3</sup>,  $K_0=0.4$ ,  $\phi=35^\circ$ ,  $\gamma_{\text{mud}}=13$  kN/m<sup>3</sup>, and  $(s_u)_{\text{FC}}=40$  kPa]

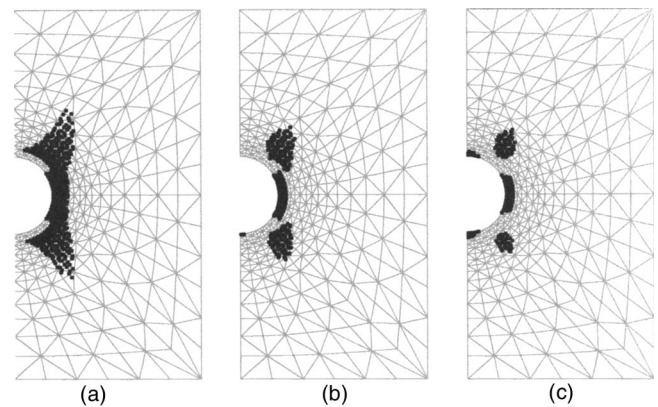


**Fig. 8.** Yielded plastic zones from finite analyses of sand-filtercake system for drilling slurry pressure of (a) 19.5; (b) 39; and (c) 52 kPa [ $h_{\text{soil}}=5$  m,  $\gamma_{\text{soil}}=20$  kN/m<sup>3</sup>,  $K_0=0.4$ ,  $\phi=35^\circ$ ,  $\gamma_{\text{mud}}=13$  kN/m<sup>3</sup>, and  $(s_u)_{\text{FC}}=40$  kPa]

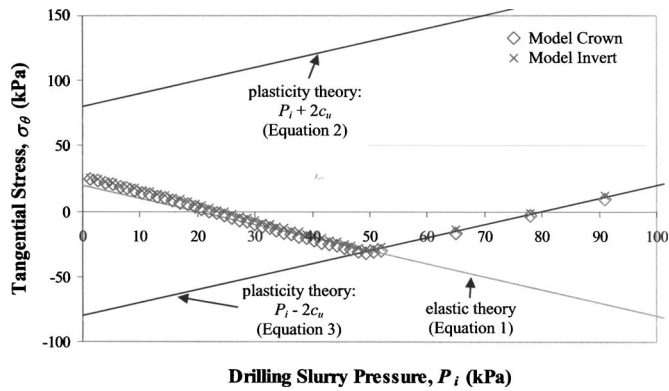


**Fig. 9.** Tangential stress at crown from elastic theory, plasticity theory, and at crown and invert from finite element analyses with a 15 cm thick filtercake layer [ $h_{\text{soil}}=5$  m,  $\gamma_{\text{soil}}=20$  kN/m<sup>3</sup>,  $K_0=0.4$ ,  $\phi=35^\circ$ ,  $\gamma_{\text{mud}}=13$  kN/m<sup>3</sup>, and  $(s_u)_{\text{FC}}=40$  kPa]

tensile strength of zero, and not to model tensile fracture or follow the fracture propagation process (a demanding exercise in computational mechanics given the well-known problems associated with localized failure). As such, it is more useful to permit tension in the analysis, to examine increases in tensile stress that result as mud pressure is increased, and the subsequent decreases in tensile stresses following shear failure in the filtercake.

Fig. 9 shows results for analyses with a 15 cm thick filtercake layer. The undrained filtercake material is relatively unaffected by the response of the sand surrounding it and behaves like the undrained clay system discussed by Kennedy et al. (2004b), where the crown stress in the analyses follows elastic theory for intermediate drilling slurry pressures, and the plasticity theory for lower and upper slurry pressures [Eqs. (1)–(3), respectively]. There are no stress changes due to shear failure in the surrounding sand, so the critical (least compressive) annular tangential stress occurs at the crown for all drilling slurry pressures.

Fig. 10 compares the tangential crown stress for varying drilling slurry pressures for analyses at a depth of five metres with 2, 7, and 15 cm thick filtercake layers. Fig. 10 indicates that the drilling slurry pressure at fracture initiation (tangential stress equal zero) is approximately 20 kPa for all these analyses. When drilling slurry pressures higher than 20 kPa are used, hydraulic

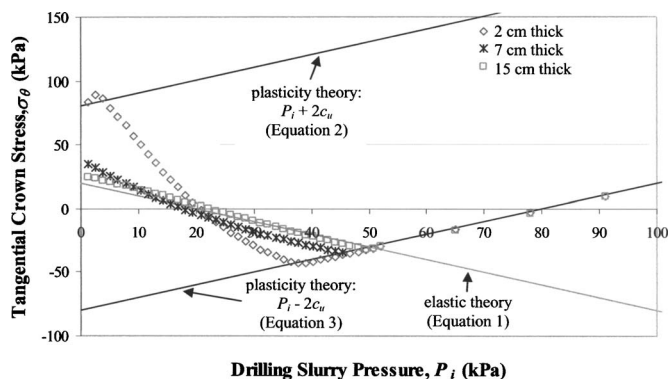


**Fig. 10.** Comparison of tangential stresses at crown for filtercake thicknesses of 2, 7, and 15 cm [ $h_{\text{soil}}=5$  m,  $\gamma_{\text{soil}}=20$  kN/m<sup>3</sup>,  $K_0=0.4$ ,  $\phi=35^\circ$ ,  $\gamma_{\text{mud}}=13$  kN/m<sup>3</sup>, and  $(s_u)_{\text{FC}}=40$  kPa]

fracture may occur. This critical slurry pressure is approximated when the elastic theory is also equal to zero, though this may be purely fortuitous.

If so, the finite element analyses of construction at a depth of 5 m indicates that a conservative estimate of the drilling slurry pressure at fracture initiation ( $P_{\text{frac}}$ ) in purely frictional sand with a purely cohesive filtercake layer can be based on elastic plate theory, Eq. (1). Although Eq. (1) provides an estimate of  $P_{\text{frac}}$  for construction at this depth, other analyses that were performed indicate that Eq. (1) may not provide conservative estimates of mud pressure corresponding to onset of tensile stresses for construction at shallower depths [for a 2 m deep borehole construction, Eq. (1) indicates onset of zero tension at a drilling slurry pressure of 8 kPa, higher than the mud pressures producing tensile stresses at both the invert or crown].

### Comparison with Design Equation for Unconfined Plastic Flow

Eq. (4) developed at the Delft University of Technology, Arends (2003), is used by designers to calculate the maximum allowable drilling slurry pressure for a specific directional drilling projects. Conroy et al. (2002) discuss two different HDD installations, 1,313 and 846 m in length, where both employed  $P_{\text{max}}$  values calculated using Eq. (4). Use of this equation in design often includes approximation of the maximum allowable radius of the plastic zone ( $R_{p,\text{max}}$ ) as half the height of soil cover for clayey and peat layers, or two-thirds of the height of soil cover for sand layers (Conroy et al. 2002; Delft Geotechnics 1997).

Comparison of the maximum allowable drilling slurry pressure calculated using this existing design equation [Eq. (4)] with the drilling slurry pressure at fracture initiation (zero tension) calculated using elastic theory [Eq. (1)] indicates that Eq. (1) provides a far more conservative estimate than Eq. (4). There is a substantial difference between these two solutions, suggesting that Eq. (1) cannot be close to the correct values, since field experience with directional drilling through sand would have produced anecdotal evidence that Eq. (4) is very unsafe.

There are at least two possible explanations. First, it could be that the tensile stress conditions seen in the previous sections are not important. This might be because any brittle failure of the ring of filtercake would allow slurry to pass through, leading to creation of an enlarged zone of filtercake. It is conceivable that the filtercake continues to reseat preventing mud loss from brittle fracture.

Alternatively, the mechanism of mud flow through fractures in the bentonite-filled sand may lead to excessive conservatism in the use of a mud pressure corresponding to initial tension. Likely, the fracture propagation process needs study to better define the mud pressures that lead to fracture-based mud loss. Research studies featuring laboratory or field simulations are likely required to establish the features of fracture propagation.

In either case, the calculation results presented here indicate that the magnitude of the mud pressures corresponding to initiation of circumferential tension are less than the head produced if the borehole pressures simply correspond to a column of drilling fluid reaching the ground surface. For instance, Figs. 7, 9, and 10 indicate that fluid pressures initiating tension are approximately 20 kPa for a borehole at 5 m depth, and these correspond to mud heights of less than half that depth. Thus, mud pressures associated with a column of fluid reaching the ground surface can be

expected to produce tensile stresses, and “posttension” behavior involving fracture rehealing or mudcake growth can be expected in the field. More study is warranted.

## Summary

Horizontal directional drilling is a construction technique that has been developed since the late 1980s to enable the installation and replacement of municipal and other buried conduits. The process involves the use of drilling slurry to aid in cooling of the head of the drill string, reduction of shear resistance along the borehole, transport of spoils, and borehole support. When drilling through a frictional host soil, a thin layer of the drilling slurry infiltrates it and creates an annulus, known as the filtercake, around the borehole.

Hydraulic fracture, a problem encountered during the HDD process, involves the loss of drilling slurry through the host soil. Two possible mechanisms of mud loss have been identified in the writers earlier work, namely flow of mud through tensile fractures in the ground, and mud loss as mud pressures induce unconfined plastic flow of the surrounding soil. When drilling through sand, the drilling mud penetrates the sand around the borehole and forms a layer of filtercake that has an important influence on the soil response. Allowable mud pressure should be selected to prevent both mud loss mechanisms.

An elastoplastic finite element model with a Mohr-Coulomb failure criterion was used to model the response of the sand-filtercake soil system, to investigate the onset of radial fracture as tangential stresses in the layer of filtercake become tensile. Directional drilling of a 0.2 m diameter borehole in medium sand was modeled at construction depths of 2 and 5 m, and featuring various thicknesses of filtercake. Comparisons were made of tangential stresses at the crown and invert of the borehole calculated using the finite element analyses, elastic plate theory, and plasticity theory for purely frictional and purely cohesive materials.

Equations based on purely frictional strength provided results for tangential stress that matched the finite element calculations for a pure sand system collapsing inward at small drilling slurry pressure, and expanding outwards at high mud pressures. Elastic plate theory calculations were made for intermediate drilling slurry pressures where sand at the crown and invert were responding elastically. However, these did not match the tangential stresses obtained using elastoplastic finite element analysis, since shear failure at other locations in the sand surrounding the borehole changed stresses at the crown or invert.

Tangential stresses in a filtercake with a 2 cm thickness were obtained using closed form plasticity calculations, and matched the finite element results at both very small and very large mud pressures. Again, elastic plate theory calculations for intermediate mud pressures where filtercake response is elastic did not match the elastoplastic finite element results, given that shear failure in the sand changed crown and invert stresses in the filtercake.

An approximate value of allowable mud pressure based on zero tangential tension was much lower than allowable mud pressures arising from an equation currently used in practice (an equation based on the prevention of unconfined plastic flow). The success of many drilling operations through sand suggests that this discrepancy in allowable mud pressure estimates results because initiation of tangential tension in the filtercake does not immediately correspond to loss of drilling mud. Further physical (laboratory) studies are warranted to investigate fracture initiation, mud flow, filtercake growth, and fracture propagation.

## References

- Allouche, E. N., Arairatnam, S. T., and Lueke, J. S. (2000). “Horizontal directional drilling: Profile of an emerging industry.” *J. Constr. Eng. Manage.*, 126(1), 68–76.
- Arairatnam, S. T., Lueke, J. S., and Allouche, E. N. (1999). “Utilization of trenchless construction methods by Canadian municipalities.” *J. Constr. Eng. Manage.*, 125(2), 76–86.
- Arends, G. (2003). “Need and possibilities for a quality push within the technique of horizontal directional drilling (HDD).” *Proc., 2003 North American No-Dig Conf.*, Las Vegas, Paper No. 36.
- Conroy, P. J., Latorre, C. A., and Wakeley, L. D. (2002). “Installation of fiber-optic cables under flood-protection structures using horizontal directional drilling techniques.” *ERDC/GSL TR-02-8*, Geotechnical Structures Laboratory, USACE.
- Delft Geotechnics. (1997). *Rep. by Department of Foundations and Underground Engineering*, prepared for O’Donnell Associates, Inc., Sugar Land, Tex.
- Edil, T. B., and Muhanna, A. S. (1992). “Characteristics of a bentonite slurry as a sealant.” *Geotech. Test. J.*, 15(1), 3–13.
- Hefhy, A., and Lo, K. Y. (1992). “The interpretation of horizontal and mixed-mode fractures in hydraulic fracturing test in rocks.” *Can. Geotech. J.*, 29, 902–917.
- Holtz, R. D., and Kovacs, W. D. (1981). *An introduction to geotechnical engineering*, Prentice-Hall, Upper Saddle River, N.J.
- Kennedy, M. J., Skinner, G. D., and Moore, I. D. (2004a). “Elastic calculations of limiting mud pressure to control hydrofracturing during HDD.” *Proc., No-Dig 2004*, New Orleans, Paper No. E-1-01.
- Kennedy, M. J., Skinner, G. D., and Moore, I. D. (2004b). “Limiting mud pressures to control hydrofracturing during HDD in an elastoplastic soil.” *Proc., 2004 Canadian Geotechnical Society Conf.*, Quebec City.
- Moore, I. D., and Booker, J. R. (1987). “Ground failure around buried tubes.” *Rock Mech. Rock Eng.*, 20(4), 243–260.
- North American Society of Trenchless Technology (NASTT). (2001). “North American Society of Trenchless Technology—About NASTT.” (<http://nastt.org/glossar/va.html>).
- Obert, L., and Duval, W. I. (1967). *Rock mechanics and the design of structures in rock*, Wiley, New York, 98–108.
- Selig, E. T. (1988). “Soil parameters for design and of buried pipelines.” *Proc., Pipeline Infrastructure Conf.*, ASCE, New York, 99–116.
- Wang, J. X., and Sterling, R. L. (2004). “Stability analysis of a borehole wall in horizontal directional drilling.” *Proc., 2004 North American No-Dig Conf.*, New Orleans, Paper No. E-1-02.